The varitint-waddler (Va) deafness mutation in TRPML3 generates constitutive, inward rectifying currents and causes cell degeneration

Keiichi Nagata*, Lili Zheng†, Thomas Madathany*, Andrew J. Castiglioni*, James R. Bartles†‡, and Jaime García-Añoveros*§¶‖

Departments of *Anesthesiology, †Cell and Molecular Biology, §Neurology, and ¶Physiology and ‡Hugh Knowles Center for Hearing Research, Northwestern University Feinberg School of Medicine, Chicago, IL 60611

Edited by Lutz Birnbaumer, National Institutes of Health, Research Triangle Park, NC, and approved November 21, 2007 (received for review August 22, 2007)

Varitint-waddler (Va and Va^J) mice are deaf and have vestibular impairment, with inner ear defects that include the degeneration and loss of sensory hair cells. The semidominant Va mutation results in an alanine-to-proline substitution at residue 419 (A419P) of the presumed ion channel TRPML3. Another allele, Va^J, has the A419P mutation in addition to an I362T mutation. We found that hair cells, marginal cells of stria vascularis, and other cells lining the cochlear and vestibular endolymphatic compartments express TRPML3. When heterologously expressed in LLC-PK1-CL4 epithelial cells, a culture model for hair cells, TRPML3 accumulated in lysosomes and in espin-enlarged microvilli that resemble stereocilia. We also demonstrated that wild-type TRPML3 forms channels that are blocked by Gd^{3+}, have a conductance of 50–70 pS and, like many other TRP channels, open at very positive potentials and thus rectify outwardly. In addition to this outward current, TRPML3(419P) and (I362T+A419P) generated a constitutive inwardly rectifying current that suggests a sensitivity to hyperpolarizing negative potentials and that depolarized the cells. Cells expressing TRPML3(A419P) or (I362T+A419P), but not wild-type TRPML3, died and were extruded from the epithelium in a manner reminiscent of degenerating hair cells in Va mice. The increased open probability of TRPML3(A419P) and (I362T+A419P) at physiological potentials likely underlies hair cell degeneration and deafness in Va and Va^J mice.

channelopathy | espin | hair cell | MCOLN3 | mucolipin

A very common cause of deafness is the loss of hair cells, which degenerate because of environmental factors or genetic mutations. Varitint-waddler (Va) mice have a mutation that causes an alanine-to-proline substitution (A419P) in the fifth transmembrane domain of TRPML3, a presumed ion channel. A second allele, Va^J, contains the A419P mutation *in cis* to an I362T mutation (1). The earliest sign of inner ear damage in Va mice is hair cell degeneration, which begins in embryogenesis as hair cells differentiate and continues postnatally. During degeneration, the hair cells bulge out of the apical side of the epithelium and become extruded. Eventually these mice also develop abnormalities in supporting cells, in the tectorial membrane, and in the stria vascularis and in the endocochlear potential that they help generate. The defects of Va^J mice are similar although less severe, suggesting that the mutation I362T attenuates the effects of A419P (1–3). A comprehensive examination of TRPML3 expression in inner ear has not been published. Expression of TRPML3 protein in hair cells was suggested by immunocytochemical methods, although results for other inner ear cell types were not reported (1).

Mutations in two other TRP channels, *Drosophila* TRP and human TRPML1 (mutations in which cause mucolipidosis type IV), are associated with degeneration of the retina. In both cases, the channels seem necessary for cellular viability, because recessive, loss-of-function mutations cause degeneration (4, 5). By contrast, the Va and Va^J mutations in TRPML3 are semidominant, although it remains unclear whether this is due to gain-of-function, haploinsufficiency, or dominant-negative effects (1, 6).

Results

We first established which cells expressed TRPML3 in the inner ear of wild-type mice. *In situ* hybridization on mouse inner ear using probes from two nonoverlapping regions of TRPML3 mRNA gave identical results [Fig. 1 and supporting information (SI) Fig. 6]. TRPML3 mRNA was most abundant in the marginal cells of the cochlear stria vascularis and the dark cells of the vestibule (Fig. 1 *i*, *l*, and *m* and SI Fig. 6 *i*, *l*, and *m*). Both cell types are involved in producing the endolymph and therefore the endocochlear potential (7–9). This expression pattern is in keeping with the reduced stria vascularis and the rounding up and loss of the cytoplasmic processes of its marginal cells in Va/Va and Va/+ mice (2) and with the reduced endocochlear potentials of the Va^J mutants (1, 3).

In addition, other cells that line the cochlear scala media and the connected vestibular endolymphatic spaces expressed TRPML3 mRNA, including (*i*) supporting cells at the marginal part of the lesser epithelial ridge (Hensen and Claudius cells), which in Va and Va^J mice (homozygotes and heterozygotes) appear undifferentiated or degenerate (Fig. 1*i* and SI Fig. 6*i*); (*ii*) cells of the spiral limbus that produce the tectorial membrane, which in Va mice develops abnormally and fails to attach to the reticular lamina (Fig. 1*i* and SI Fig. 6*i*); (*iii*) cells of the spiral ligament (Fig. 1*i* and SI Fig. 6*i*); and (*iv*) cells of the Reissner's membrane (Fig. 1*i* and SI Fig. 6*i*). Importantly, TRPML3 mRNA was also detected in the sensory hair cells of the vestibular system and cochlea (Fig. 1 *a*, *e*, *i*, *n*, and *p* and SI Fig. 6 *a*, *e*, *i*, *n*, and *p*), which degenerate in Va and Va^J mice (1–3).

Our detection of TRPML3 mRNA in hair cells supported immunostaining evidence suggesting that TRPML3 is expressed in hair cells (1). We expressed a TRPML3::GFP fusion protein heterologously in LLC-PK1-CL4 epithelial (CL4) cells, a culture model of hair cells (10). CL4 cells heterologously expressing the actin-bundling protein espin elongate their microvilli to resemble hair cell stereocilia, and indeed several heterologously

Author contributions: J.R.B. and J.G.-A. designed research; K.N., L.Z., A.J.C., and J.R.B. performed research; T.M. and A.J.C. contributed new reagents/analytic tools; K.N., L.Z., J.R.B., and J.G.-A. analyzed data; and J.R.B. and J.G.-A. wrote the paper.

The authors declare no conflict of interest.

This article is a PNAS Direct Submission.

Freely available online through the PNAS open access option.

‖To whom correspondence should be addressed at: Ward 10-070, 303 East Chicago Avenue, Chicago, IL 60611. E-mail: anoveros@northwestern.edu.

This article contains supporting information online at www.pnas.org/cgi/content/full/0707963105/DC1.

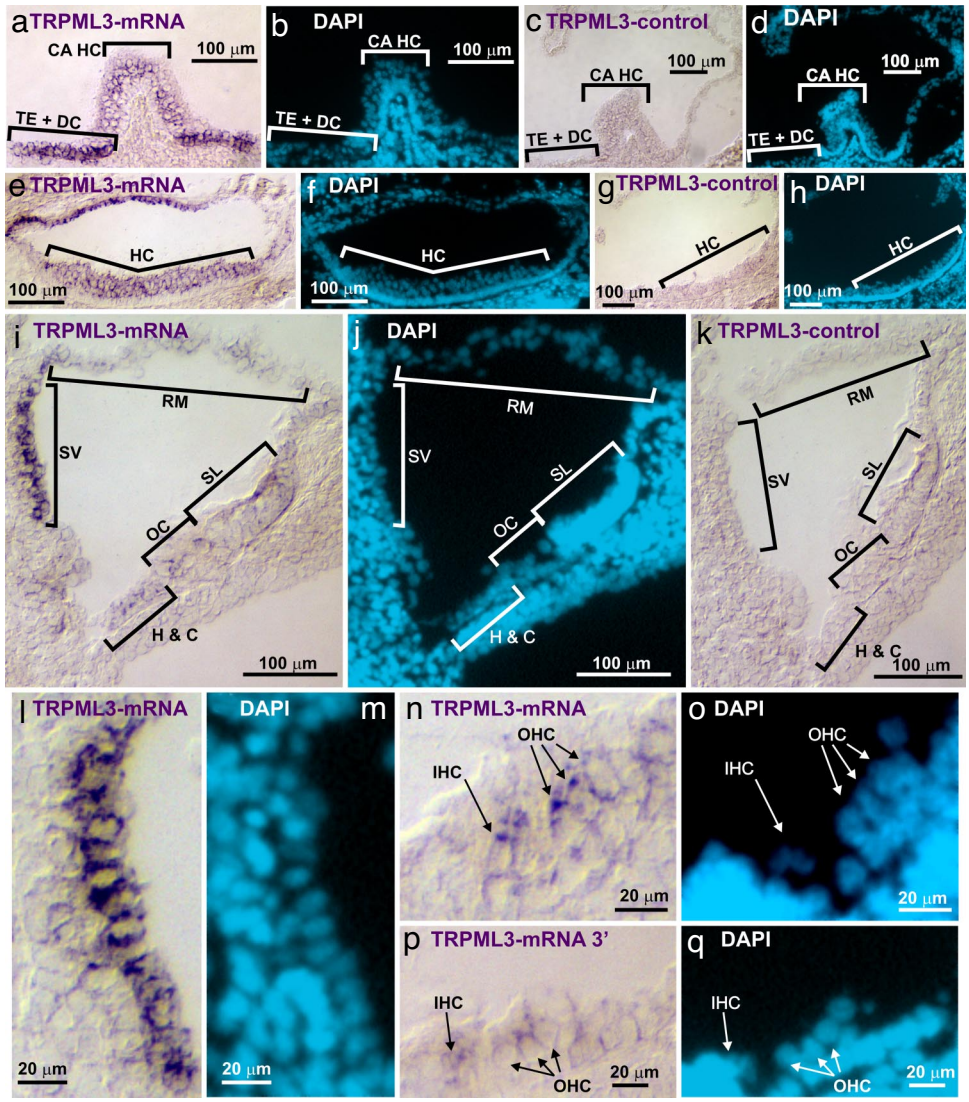

Fig. 1. Expression of TRPML3 mRNA in hair cells, stria vascularis, Reissner's membrane, and other cells lining the scala media of the cochlea and the endolymphatic spaces of the vestibule. *In situ* hybridization with antisense probes to the 3′ half of TRPML3 mRNA (*a*, *e*, *i*, *l*, *n*, and *p*), control with sense probes (*c*, *g*, and *k*) and nuclear DAPI label (*b*, *d*, *f*, *h*, *j*, *m*, *o*, *q*). (*a*–*d*) Crista ampullaris: TRPML3 in vestibular hair cells (CA HC) and adjacent transient epithelium and dark cells (TE+DC). (*e*–*h*) Sacculus: TRPML3 in vestibular hair cells (HC) and in cells of the vestibular membrane. (*i*–*k*) Cochlear scala media: TRPML3 in stria vascularis (SV), Reissner's membrane (RM), spiral limbus (SL), hair cells of the organ of Corti (OC), and support cells of the marginally located lesser epithelial ridge (H & C, Hensen's and Claudius' cells). (*l* and *m*) Marginal cells of the stria vascularis express TRPML3 mRNA. (*n*–*q*) Cochlear inner and outer hair cells (IHC and OHC) express TRPML3 mRNA. All sections are from P5 mice.

expressed stereociliary proteins localize to these espin-enlarged microvilli (10) (L.Z., J.G.-A. and J.R.B., unpublished work). Heterologously expressed TRPML3::GFP localized to intracellular vesicles and to espin-enlarged microvilli (Fig. 2 *a*–*d*), resembling the localization to hair cell vesicles and stereocilia observed with antibodies to TRPML3 (1). The large cytoplasmic vesicles appeared to be lysosomes, because they labeled with the endocytic pathway marker Texas red-dextran (70 kDa) after a 1-h pulse and a prolonged (4- to 6-h) chase (11, 12) (SI Fig. 7 *a*–*c*). Small amounts of TRPML3::GFP were also detected in endoplasmic reticulum, which we colabeled with DsRed2-ER (a fusion of DsRed2 with the ER targeting signal of calreticulin; SI Fig. 7 *d*–*f*). However, some of the TRPML3::GFP was clearly at the plasma membrane, because large TRPML3 currents were recorded from the transfected CL4 cells (see below; Fig. 3 *i* and *j*).

The earliest phenotype of Va and Va^{J} mice appears to be hair cell degeneration, which begins during embryogenesis, days before the formation of the endolymph (1, 3). Specifically, hair cells in Va and Va^{J} mice loose their columnar epithelial appearance, round up, bulge out of the epithelium and are extruded from it (2, 3). We found that CL4 cells expressing TRPML3(A419P) degenerated in a strikingly similar manner (Fig. 3 *a*–*h*). Twenty-four hours after transfection, most CL4 cells expressing TRPML3(A419P) (77 ± 2%) or TRPML3(I362T+A419P) (78 ± 6%) became extruded from the epithelial monolayer and took up the cell death marker propidium iodide, whereas adjacent untransfected cells did not. By comparison, almost no CL4 cells expressing wild-type TRPML3 (3 ± 1%) or TRPML3(I362T) (2 ± 1%) died (mean ± SD; three independent experiments; 200–250 transfected cells of each type were examined per experiment). Hence, TRPML3(A419P) causes a form of cell-autonomous cell death that could account for the hair cell degeneration and loss in Va and Va^{J} mice. We next wondered how the A419P substitution caused cell death.

To examine the physiological properties of TRPML3, we recorded from CL4 and HEK 293 cells that heterologously

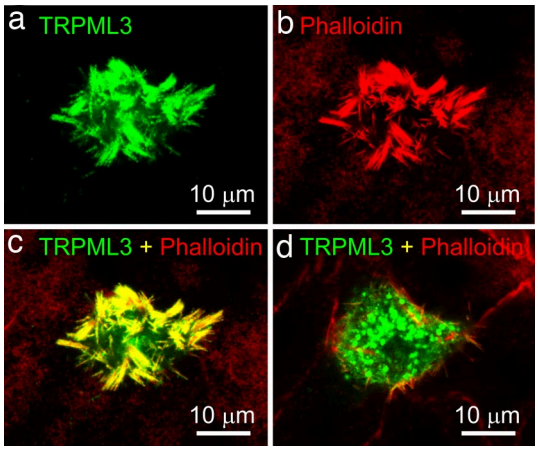

Fig. 2. Localization of TRPML3::GFP in LLC-PK1-CL4 cells. (*a–d*) CL4 cells coexpressing TRPML3::GFP (green) and espin, which results in enlarged microvilli that resemble hair cell stereocilia. Phalloidin (red) labels F-actin. (*a–c*) Optical section through apical end of cell demonstrating localization of (*a*) TRPML3 to (*b*) enlarged microvilli (merged in *c*). (*d*) Optical section through the cell body demonstrating localization of TRPML3 to intracellular vesicles.

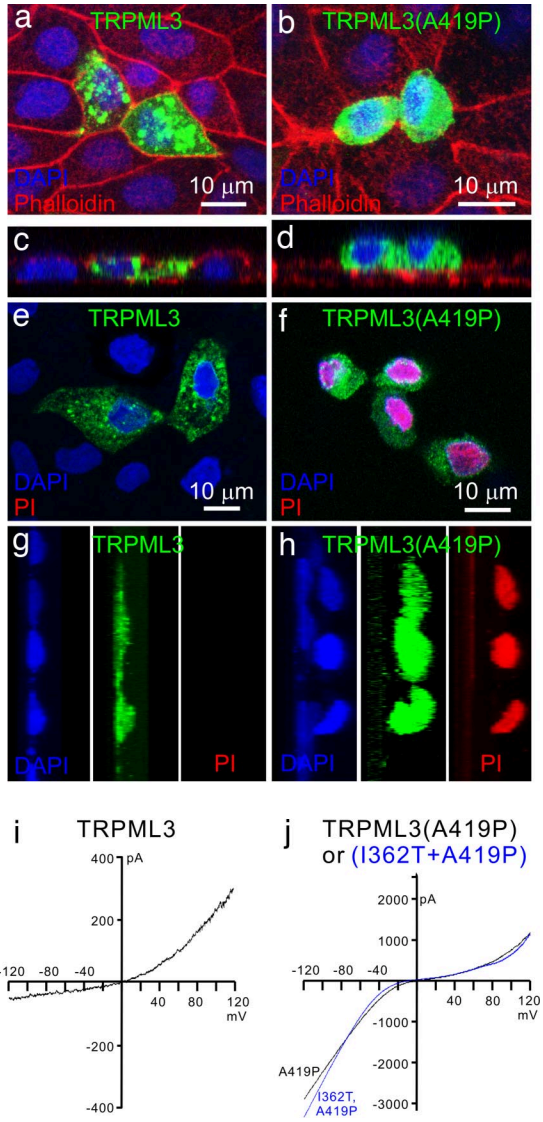

Fig. 3. Extrusion and death of LLC-PK1-CL4 cells expressing TRPML3(A419P). (*a* and *c*) Cells expressing wild-type TRPML3 remain in the epithelium. (*b* and *d*) Cells expressing TRPML3(A419P) round up and become extruded from the epithelium. (*a* and *b*) Top views. (*c* and *d*) Orthogonal (*x* and *z*) sections. (*f* and *h*) Cells expressing TRPML3(A419P) take up the cell death marker propidium iodide (PI), whereas (*e* and *g*) cells expressing wild-type TRPML3 do not. The optical section in *f* cuts through the transfected cells, above the monolayer of untransfected cells. (*e* and *f*) Top views. (*g* and *h*) Lateral 3D projections. There was a 1:1 correlation between epithelial extrusion and PI uptake. DAPI labels nuclei and phalloidin F-actin. (*i* and *j*) TRPML3 currents in CL4 cells demonstrate channel expression in their plasma membrane. (*i*) Current–voltage (IV) plot of CL4 cells expressing TRPML3::GFP. (*j*) IV plot of CL4 cells expressing TRPML3(A419P)::GFP or TRPML3(I362T+A419P)::GFP, both of which add an inwardly rectifying current. Identical currents were obtained in HEK 293 cells expressing these constructs or untagged ones (Fig. 4). The currents found in CL4 cells expressing TRPML3 ($n = 8$), TRPML3(A419P) ($n = 8$), or TRPML3(I362T+A419P) ($n = 4$) were not detected in untransfected CL4 cells ($n = 6$).

expressed TRPML3 (Figs. 3 *i* and *j*, 4, and 5). The physiology of TRPML3 channels has not been examined previously, and there are no known agonists of TRPML3 channels. However, many other TRP channels have a voltage sensitivity that leaves them open at positive membrane potentials (13–16). Therefore, we tested whether voltage also activated TRPML3 channels. Indeed, cells heterologously expressing TRPML3 exposed to voltage ramps showed outwardly rectifying currents that were blocked by gadolinium (Gd^{3+}), a blocker of other TRP channels (Figs. 3, 4 *a* and *c*, and 5*a*). These outwardly rectifying currents were not affected by removal of divalent cations, and thus this rectification is not due to voltage-sensitive block. The pronounced outward rectification observed in whole cells was not due to increased single-channel conductance. Patch recordings reveal a linear single-channel conductance of 50 pS (at negative voltages) to 70 pS (at positive voltages) (Fig. 5*c*). However, voltage ramps reveal that TRPML3 channels open primarily at positive voltages (Fig. 5*a*). Thus, the outward rectification of TRPML3, like that of other TRP channels (13–16), is probably due to a voltage-sensitive increase in open probability (Fig. 4*b*).

To elucidate the effects of the degeneration-causing A419P mutation on TRPML3 channels, we recorded currents from CL4 and HEK 293 cells and membrane patches heterologously expressing TRPML3(A419P) or TRPML3(I362T+A419P). Although these cells displayed the outwardly rectifying currents characteristic of wild-type TRPML3, they had an additional and very large inwardly rectifying current at negative voltages (Figs. 3*j* and 4 *a* and *c*). This mutant inward current was also blocked by Gd^{3+}, with an IC_{50} similar to that for the outward currents of both mutant and wild-type TRPML3 (Fig. 4*e*). From reversal potential measurements, we estimate that TRPML3(A419P) is equally permeable to Na^+ and K^+ and more permeable to Ca^{2+} ($P_{Ca^{2+}}/P_{Na^+} = 67 \pm 37$; $n = 4$ cells), although the conductance is greater for monovalent ions than for Ca^{2+} (Fig. 4*f*).

Two potential mechanisms by which a channel could display inward rectification are if it selects preferentially for Ca^{2+} or its outward currents are blocked by Mg^{2+}. However, the inwardly rectifying current of cells expressing TRPML3(A419P) was also present in the absence of divalent cations from both the external and internal solutions (Fig. 4*d* and data not shown). Thus, the inward rectification of the mutant channel is not due to a preferential permeation of, or block by, divalent cations. Another mechanism by which a channel may display inward rectification is if its conductance is larger at negative potentials. However, single-channel recordings from outside-out patches of membrane revealed the same linear single-channel conductance for wild-type and A419P mutant TRPML3 channels: ≈50 pS at negative potentials and up to 70 pS in the positive range (Fig. 5*c*). Hence, the A419P mutation does not generate inwardly rectifying currents by altering their single-channel conductance.

NEUROSCIENCE

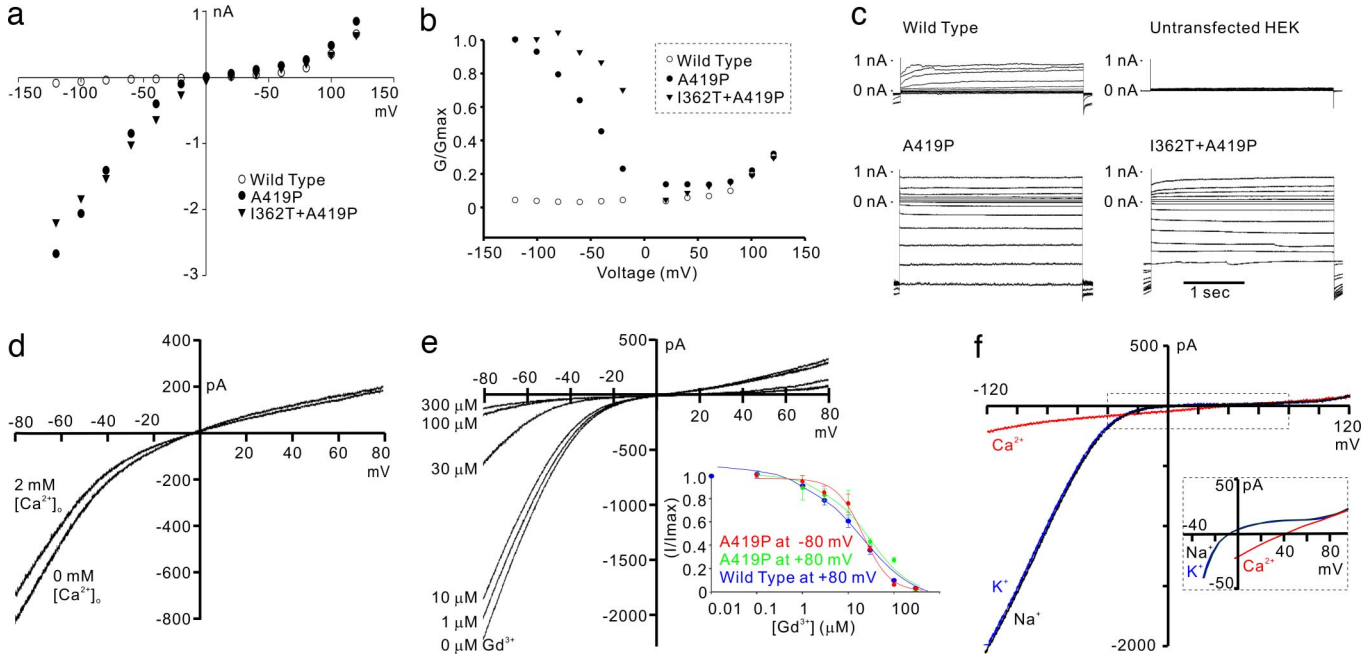

Fig. 4. The degeneration causing A419P mutation results in depolarization-sensitive opening of TRPML3 channels at negative voltages. (*a*) IV plot of cells expressing TRPML3, TRPML3(A419P), or TRPML3(I362T+A419P) shows outward currents at positive potentials in wild type and mutants and an additional inward current at negative potentials in mutants. (*b*) Apparent open probabilities (G/Gmax) at various voltages. The A419P mutation (with or without I362T) does not affect the increase of channel opening with membrane potential increases in the positive voltage range, but induces opening at hyperpolarized negative voltages. Gmax is defined as the steady-state conductance of TRPML3(A419P) or (I362T+A419P) at −120 mV. G is the steady-state conductance at the plotted membrane potentials. (*c*) Whole-cell currents elicited by voltage steps from −120 mV to up to +120 mV. A use-dependent increase in current at −120 mV was detected in cells expressing mutant or wild-type TRPML3. (*d*) IV plots cells expressing TRPML3(A419P) demonstrating that inward rectification is not affected by the presence or absence of external Ca^{2+}. External solution with 0 mM Ca^{2+} contained 4 mM EGTA. Both external solutions lacked Mg^{2+}. (*e*) IV plots of cells expressing TRPML3(A419P) showing block by Gd^{3+}. (*Inset*) Dose–responses indicate that block is independent of voltage and unaffected by the A419P mutation [IC_{50} of TRPML3(A419P) at −80 mV is 20.6 ± 2.0 μM; IC_{50} of TRPML3(A419P) at +80 mV is 24.6 ± 6.7 μM; IC_{50} of wild-type TRPML3 at +80 mV is 14.8 ± 2.5 μM; $n = 3$ or 4]. (*f*) IV plots of cells expressing TRPML3(A419P) in the presence of external solutions containing either 140 mM NaCl, 140 mM KCl, or 20 mM $CaCl_2$ plus 98 mM NMDGCl. The reversal potential was near 0 mV with Na^+ or K^+, but more positive with Ca^{2+} (there were no inward currents with 140 mM NMDGCl externally, from which we deduce that neither Cl^- nor $NMDG^+$ permeate). Cells were HEK 293T.

Instead, TRPML3(A419P) channels appear to generate inwardly rectifying currents by increasing open probability at negative voltages (Figs. 4*b* and 5*b*). The outward rectification characteristic of many TRP channels, including wild-type TRPML3, results from a weak voltage sensitivity: Open probability increases with "depolarization" at positive membrane potentials, in the nonphysiological range (13–16) (Fig. 4*b*). Activation of some of these TRP channels by physical stimuli such as temperature or by ligand binding shifts their voltage sensitivity toward negative potentials, so that channels open in the physiological range of membrane resting potentials (13–16). However, these channels still display outward rectification, because their open probability increases with depolarization. By contrast, the A419P mutation in TRPML3 does not alter the voltage sensitivity of its outwardly rectifying current (Fig. 4*b*). Instead, this mutation induces another, inwardly rectifying current in which whole-cell conductance and channel apparent open probability increase with hyperpolarization and decrease with depolarization (Fig. 4*b*). The A419P-activated TRPML3 channel appears to be gated by different voltage-sensitivities at positive and negative potentials.

The result of the A419P-induced inward rectification is a constitutive inward current at normal cellular resting potentials. Accordingly, CL4 cells expressing TRPML3(A419P) channels and displaying these constitutive currents became completely depolarized. Although the resting membrane potential of untransfected CL4 cells was −26.3 ± 3.6 mV (n = 7) and that of CL4 cells expressing wild-type TRPML3 was −24.8 ± 3.3 mV (n = 6), CL4 cells expressing TRPML3(A419P) were depolarized to 1.3 ± 1.1 mV (n = 3), as expected for cells expressing leak cationic currents. This depolarization was measured in live cells (without leaky plasma membranes) and therefore occurred before cell death, not as a consequence of it.

Discussion

We have demonstrated that the TRPML3 mRNA is expressed in hair cells and that the channels formed by the TRPML3 protein are activated by the A419P mutation to generate constitutive currents at normal physiological resting potential. Very positive potentials, not reached by cells in physiological conditions, can open several TRP channels, including TRPML3. Stimuli like temperature or chemical agonists open some of these TRP channels by shifting this voltage sensitivity toward negative potentials, into the physiological range. By contrast, the A419P mutation does not affect the voltage sensitivity of TRPML3 at positive potentials but instead appears to open the channel at negative potentials with a reversed voltage sensitivity (increased open probability by voltage changes toward negative, rather than positive, voltages). It remains to be determined whether there are physiological forms of stimulation that can open TRPML3 in the same way than the A419P mutation does or whether they activate by shifting the voltage sensitivity of TRPML3 to "depolarizations" (i.e., voltage changes toward positive, or less negative, potentials).

When expressed in the CL4 epithelial cell model, both TRPML3(A419P) and TRPML3(I362T+A419P) resulted in severe depolarization, extrusion from the monolayer and cell

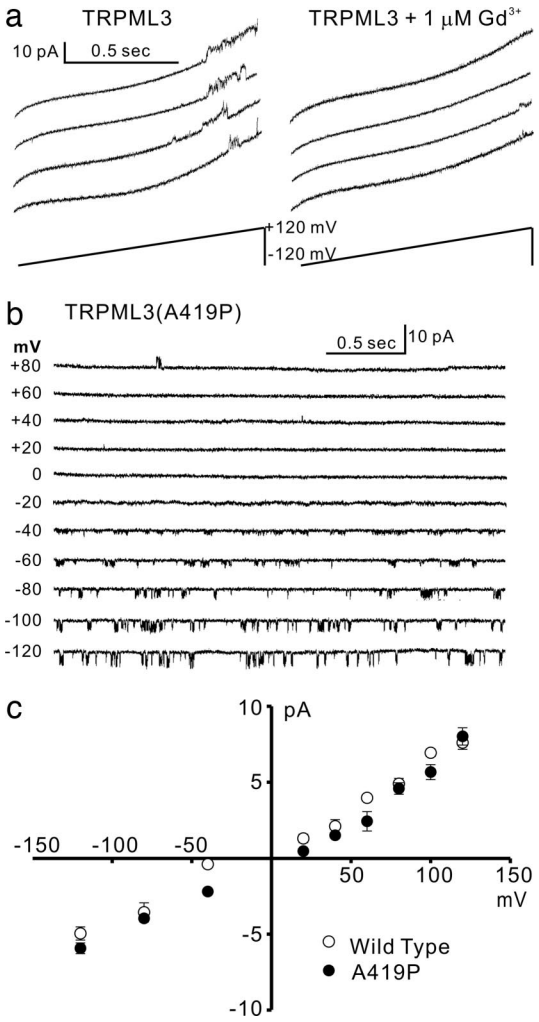

Fig. 5. Single-channel currents of TRPML3 and TRPML3(A419P). (*a*) Voltage ramps of outside-out membrane patches from cells expressing TRPML3 reveal preferential channel opening at positive potentials and block by Gd^{3+}. (*b*) Voltage steps of an outside-out membrane patch from a cell expressing TRPML3(A419P) reveal increased channel opening at negative potentials. (*c*) IV plots of single-channel current amplitudes show the same single-channel conductance for TRPML3 and TRPML3(A419P).

death. Because these defects resemble the fate of hair cells in Va and Va^J mice, we propose that this A419P mutation-induced change in TRPML3 physiology underlies the hair cell degeneration and loss observed in deaf Va and Va^J mice. Although Va^J mice have a weaker phenotype than Va mice, we did not detect any difference in the lethality of cells expressing TRPML3(A419P) and TRPML3(I362T+A419P). This explains why Va^J mice also exhibit hair cell degeneration and deafness but not why this allele is less severe than Va. Perhaps the mechanism of attenuation requires endogenous conditions or cofactors lacking in heterologous CL4 cells.

Constitutive channel activation has been implicated in other inherited forms of neurodegeneration. This phenomenon was first reported in the degenerin channels of *Caenorhabditis elegans* (17–19) in which gain-of-function mutations that increase channel open probability cause cellular degeneration of both endogenously expressing neurons and of heterologously expressing cells (20, 21). Like we found for TRPML3(A419P), the mutated nematode degenerin channels also caused constitutive cationic currents, which result in complete depolarization (to near 0 mV resting membrane potential) and cell death (20). However, although there are mammalian homologs of nematode degenerins that when similarly mutated also kill heterologously expressing cells (22, 23), there are, to date, no disorders caused by mutations in these channels. Other cell degeneration-causing mutations occur in a nematode acetylcholine receptor (24, 25) and in the mouse δ2 orphan glutamate receptor (mutated in the Lurcher mouse) (26, 27). To our knowledge, the Va and Va^J mutations provide the first examples of a cellular degeneration channelopathies involving constitutive activation of a mammalian TRP channel.

A common interpretation for these degenerative channelopathies is that excessive cation influx through the plasma membrane causes lethal levels of $[Ca^{2+}]_i$ or of depolarization. The same might explain death caused by TRPML3(A419P). However, the presence of TRPML3 in lysosomal vesicles raises the possibility that the lethal effects of the mutant channels are due, in full or in part, to their effects on these organelles. Indeed, a number of neurodegenerative conditions are caused by defective lysosomal storage (28). In either case, the hyperactivity caused by A419P is the likely cause of the hair cell degeneration in Va and Va^J mice. The semidominance of the Va mutation has been proposed to result from a gain of function, a partial loss of function, or a dominant-negative effect of the A419P substitution (1, 6). Our results indicate that the Va mutation acts as a gain of function.

We describe a form of deafness caused by a channelopathy of a TRP channel. TRP channels mediate hearing in invertebrates, and there is much interest in figuring out whether they play a similar role in vertebrates. The expression of TRPML3 in hair cells, its likely localization to stereocilia, and some of its properties, like the block by gadolinium, suggest a potential contribution of this channel protein to hair cell transduction. On the other hand, the high expression of TRPML3 in lysosomal vesicles and its homology to, and capacity to interact with, the lysosomal channels TRPML1 and TRPML2 (29) are also consistent with roles in intracellular membranes. Regardless of the function of wild-type TRPML3, it is clear that it causes deafness when bearing a mutation (A419P) that generates constitutive currents.

Methods

***In Situ* Hybridization.** *In situ* hybridization was performed as described (30). To confirm specificity, we hybridized with either of two nonoverlapping RNA probes corresponding to fragments of TRPML3 mRNA. Experimental details are provided in *SI Methods*.

Cell Culture and Heterologous Expression. LLC-PK1-CL4 epithelial cells were cultured on glass coverslips, transfected by using lipofectamine and examined by confocal microscopy, with and without labeling for F-actin with Texas red-phalloidin, as described (10). The nuclei of fixed cells were labeled with DAPI, and cell death was assayed by uptake of propidium iodide upon incubation for 4 min in 2.5 μg/ml propidium iodide in PBS before a brief rinse and fixation. HEK 293 cells were transiently transfected with TRPML3 cDNA constructs by lipofectamine 2000. HEK 293 or LLC-PK1-CL4 cells were used for patch–clamp experiments 24 h after transfection.

TRPML3 mammalian expression constructs contain the full-length mouse TRPML3 cDNA under a CMV promoter and either GFP under the control of a separate promoter (vector pHGCX) or as a C-terminal fusion with TRPML3 (vector pEGFP-N2). Approximately 24 h after transfection, we select cells for recording based on GFP fluorescence. In some experiments, cells were cotransfected with mammalian expression constructs for espin (pcDNA3-rat espin 2B) or with DsRed2-ER (Clontech) or incubated for 1 h with 1 mg/ml Texas red-Dextran (70 kDa; Molecular Probes).

Electrophysiological Recordings. Electrophysiological recordings of whole cells and single channels were performed as described (30). Detailed protocols are provided in *SI Methods*.

ACKNOWLEDGMENTS. This work was supported by National Institutes of Health Grants NS044363 (to J.G.-A.), DC004314 (to J.R.B.), and Training Grant T32 NS041234 (to A.J.C.).

1. Di Palma F, Belyantseva IA, Kim HJ, Vogt TF, Kachar B, Noben-Trauth K (2002) *Proc Natl Acad Sci USA* 99:14994–14999.
2. Deol MS (1954) *J Genet* 52:562–588.
3. Cable J, Steel KP (1998) *Hear Res* 123:125–136.
4. Nilius B, Owsianik G, Voets T, Peters JA (2007) *Physiol Rev* 87:165–217.
5. Wang T, Montell C (2007) *Pflugers Arch* 454:821–847.
6. Lester HA, Karschin A (2000) *Annu Rev Neurosci* 23:89–125.
7. Wangemann P (1995) *Hear Res* 90:149–157.
8. Vetter DE, Mann JR, Wangemann P, Liu J, McLaughlin KJ, Lesage F, Marcus DC, Lazdunski M, Heinemann SF, Barhanin J (1996) *Neuron* 17:1251–1264.
9. Wangemann P, Schacht J (1996) in *The Cochlea*, eds Dallos P, Popper AN, Fay RR (Springer, New York), pp 130–186.
10. Loomis PA, Zheng L, Sekerkova G, Changyaleket B, Mugnaini E, Bartles JR (2003) *J Cell Biol* 163:1045–1055.
11. Baravalle G, Schober D, Huber M, Bayer N, Murphy RF, Fuchs R (2005) *Cell Tissue Res* 320:99–113.
12. Thilo L, Stroud E, Haylett T (1995) *J Cell Sci* 108 (Pt 4):1791–1803.
13. Nilius B, Talavera K, Owsianik G, Prenen J, Droogmans G, Voets T (2005) *J Physiol* 567:35–44.
14. Voets T, Droogmans G, Wissenbach U, Janssens A, Flockerzi V, Nilius B (2004) *Nature* 430:748–754.
15. Brauchi S, Orio P, Latorre R (2004) *Proc Natl Acad Sci USA* 101:15494–15499.
16. Latorre R, Brauchi S, Orta G, Zaelzer C, Vargas G (2007) *Cell Calcium* 42:427–438.
17. Chalfie M, Wolinsky E (1990) *Nature* 345:410–416.
18. Driscoll M, Chalfie M (1991) *Nature* 349:588–593.
19. García-Añoveros J, Ma C, Chalfie M (1995) *Curr Biol* 5:441–448.
20. García-Añoveros J, Garcia JA, Liu JD, Corey DP (1998) *Neuron* 20:1231–1241.
21. Goodman MB, Ernstrom GG, Chelur DS, O'Hagan R, Yao CA, Chalfie M (2002) *Nature* 415:1039–1042.
22. Waldmann R, Champigny G, Voilley N, Lauritzen I, Lazdunski M (1996) *J Biol Chem* 271:10433–10436.
23. García-Añoveros J, Derfler B, Neville-Golden J, Hyman BT, Corey DP (1997) *Proc Natl Acad Sci USA* 94:1459–1464.
24. Treinin M, Chalfie M (1995) *Neuron* 14:871–877.
25. Treinin M, Gillo B, Liebman L, Chalfie M (1998) *Proc Natl Acad Sci USA* 95:15492–15495.
26. Zuo J, De Jager PL, Takahashi KA, Jiang W, Linden DJ, Heintz N (1997) *Nature* 388:769–773.
27. Kohda K, Wang Y, Yuzaki M (2000) *Nat Neurosci* 3:315–322.
28. Vellodi A (2005) *Br J Haematol* 128:413–431.
29. Venkatachalam K, Hofmann T, Montell C (2006) *J Biol Chem* 281:17517–17527.
30. Nagata K, Duggan A, Kumar G, García-Añoveros J (2005) *J Neurosci* 25:4052–4061.